

# Coherent perfect absorption of single photons in a fiber network

Cite as: Appl. Phys. Lett. **115**, 191101 (2019); doi: [10.1063/1.5118838](https://doi.org/10.1063/1.5118838)

Submitted: 6 July 2019 · Accepted: 22 October 2019 ·

Published Online: 4 November 2019






View Online



Export Citation



CrossMark

Anton N. Vetlugin,<sup>1,a)</sup>  Ruixiang Guo,<sup>1</sup>  Angelos Xomalis,<sup>2</sup>  Salih Yanikgonul,<sup>1,3</sup>  Giorgio Adamo,<sup>1</sup>  Cesare Soci,<sup>1,a)</sup>  and Nikolay I. Zheludev,<sup>1,2</sup> 

## AFFILIATIONS

<sup>1</sup>Centre for Disruptive Photonic Technologies, SPMS, TPI, Nanyang Technological University, Singapore 637371, Singapore

<sup>2</sup>Optoelectronics Research Centre and Centre for Photonic Metamaterials, University of Southampton, Southampton SO17 1BJ, United Kingdom

<sup>3</sup>Advanced Optical Technologies, Institute of Materials Research and Engineering, Agency for Science, Technology and Research, Singapore 138634, Singapore

<sup>a)</sup>Authors to whom correspondence should be addressed: [a.vetlugin@ntu.edu.sg](mailto:a.vetlugin@ntu.edu.sg) and [csoci@ntu.edu.sg](mailto:csoci@ntu.edu.sg)

## ABSTRACT

Large distance implementation of quantum communication technologies requires coherent control of single photons in optical fiber networks. Here we demonstrate the phenomenon of coherent perfect absorption of single photons in a fully fiberized ultrathin plasmonic metamaterial fabricated at the end facet of an optical fiber. Continuous control of single-photon absorption probability is achieved by driving the network between the regimes of coherent total absorption and coherent total transmission. To circumvent phase fluctuations inherent to optical fiber networks, we implemented a reference-based postselection technique which yielded interference fringe visibility comparable to that of free space experiments. Coherent absorption of quantum light in fiber environment provides new opportunities for dissipative single-photon switching, filtering, and measurement, as well as for manipulation of entangled, weak coherent, and NOON states in optical fiber networks.

Published under license by AIP Publishing. <https://doi.org/10.1063/1.5118838>

Coherent interaction of light beams in the presence of a subwavelength absorber allows us to achieve regimes of coherent total absorption or coherent total transmission, without requiring intrinsic nonlinearity.<sup>1</sup> Reflection, absorption, and transmission parameters necessary to achieve these regimes, however, are not easily accessible with natural materials, but they can be reached by artificial nanostructuring. It was demonstrated that plasmonic ultrathin metamaterials provide nonlinear input-output signal dependencies<sup>2</sup> and may be coherently controlled with multiterahertz bandwidth,<sup>3</sup> and without introducing signal distortion at very low intensity, down to the single photon level. The latter was used to extend the coherent perfect absorption (CPA) phenomenon to the quantum regime with manipulation of pure single-photon,<sup>4</sup> entangled<sup>5</sup> and NOON<sup>6</sup> states with a potential to control continuous-wave quantum states<sup>7</sup> as well. We note that CPA was demonstrated also as an effective approach to transfer light energy to other light-matter eigenstates such as exciton-polaritons<sup>8</sup> and magnon-polaritons<sup>9</sup> with a promise to bring phenomena of quantum optics to different platforms.<sup>10</sup>

Application of CPA in practical light processing and communication, both in classical and quantum regimes, requires implementation in optical fiber environment, with an access to mainstream telecom technologies. Deep subwavelength thickness of metamaterial absorbers makes them suitable for such implementation. Indeed, an encapsulated plasmonic metamaterial (metadevice) was recently shown to operate all-optical switching and logical functions in the C-band of a telecom fiber network.<sup>11</sup> In this demonstration, the operation frequency (from 20 kHz up to 40 GHz) was a few orders of magnitude higher than the characteristic phase fluctuation frequency of the fiber network ( $\sim$ Hz); thus, no phase stabilization was required. However, realization of CPA at a single photon level is hindered by the low photon flux, which is incompatible with high signal modulation frequency. Techniques like fiber network stabilization or data postselection processing are required in this case.

Here we show coherent interaction of light at single photon state on a plasmonic metamaterial performed in a fully fiberized quantum network. We built a network based on an optical fiber Mach-Zehnder

interferometer containing a fiber-packaged plasmonic metadvice. By exploiting access to both coincidence and single-photon counts information and using advanced data postselection procedure, we overcome the fiber stabilization problem. In this network, we demonstrate the quantum regimes of coherent perfect transmission and coherent perfect absorption with a subwavelength lossy beam splitter in fiber environment, thereby providing an important step toward quantum light manipulation with direct implementation in fiberized quantum systems.

To introduce quantum regimes of perfect absorption and perfect transmission, let us consider an ultrathin lossy beam splitter, or absorber, that produces a  $\pi$ -phase shift between transmitted and reflected fields.<sup>4,12</sup> If such beam splitter is interrogated with a single photon, whose wavefunction is split beforehand and recombined at the beam splitter, the phase shift  $\varphi$  between two “parts” of the photon’s wavefunction (defined at the metamaterial position) gives rise to two possible, and opposite, outcomes. Constructive interference occurs when  $\varphi = \pm\pi$ , with the photon passing through the absorber without any losses. Conversely, destructive interference occurs when  $\varphi = 0$  since reflected and transmitted fields cancel each other and the photon is fully dissipated (absorption probability under coherent illumination reaches unity if absorption of the beam splitter for a traveling wave is 50%). These two limited cases are known as coherent perfect transmission and coherent perfect absorption, respectively. In more detail, the quantum state of the photon under consideration is described by the path-entangled wave function

$$|\psi\rangle = \frac{1}{\sqrt{2}} (|1\rangle_A |0\rangle_B + e^{i\varphi} |0\rangle_A |1\rangle_B), \quad (1)$$

where index  $A(B)$  corresponds to the top (bottom) input field of the absorber in Fig. 1(a) and is related to the annihilation operator  $\hat{a}$  ( $\hat{b}$ ), satisfying commutation relations,  $[\hat{a}, \hat{a}^\dagger] = [\hat{b}, \hat{b}^\dagger] = 1$ ,  $[\hat{a}, \hat{b}^\dagger] = 0$ . The wave function  $|\psi\rangle$  also contains controllable relative phase shift  $\varphi$ , which is accumulated during propagation through two optical passes to the absorber. A thin lossy beam splitter mixes the input amplitudes and adds the Langevin noise operators  $\hat{f}_c$  and  $\hat{f}_d$  which are responsible for commutation relation conservation<sup>13,14</sup>

$$\hat{c} = t\hat{a} + r\hat{b} + \hat{f}_c, \quad \hat{d} = r\hat{a} + t\hat{b} + \hat{f}_d.$$

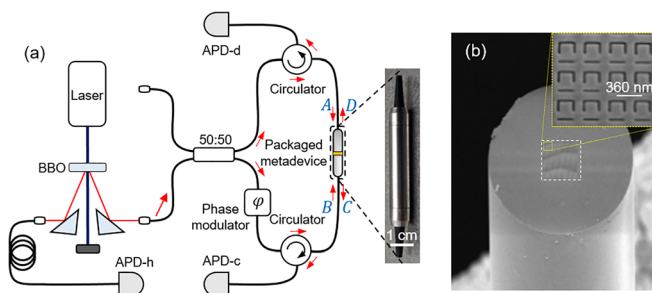


**FIG. 1.** Coherent perfect absorption in a quantum network. (a) Schematic of the fiberized quantum network with a plasmonic metamaterial absorber and heralded single photon source. Red arrows mark heralded single photon path. The inset shows a photograph of the packaged metadvice. (b) SEM image of the plasmonic metamaterial absorber deposited on the end-facet of an optical fiber. The inset shows the SEM image of the nanostructure.

Here  $\hat{c}$  ( $\hat{d}$ ) is the annihilation operator related to the bottom (top) output field of the absorber in Fig. 1(a), and  $t$  ( $r$ ) is the amplitude transmission (reflection) coefficient for traveling waves. It is straightforward to calculate the probabilities  $p_c$  and  $p_d$  of detecting a photon at the corresponding output ports of the absorber, which, in the case of a single photon input state and unitary detection efficiency, equal the mean values of the photon number operators

$$p_c = \langle \hat{c}^\dagger \hat{c} \rangle = (|t|^2 + |r|^2 + 2|t||r|\cos(\varphi - \Delta_{tr}))/2, \quad (2)$$

$$p_d = \langle \hat{d}^\dagger \hat{d} \rangle = (|t|^2 + |r|^2 + 2|t||r|\cos(\varphi + \Delta_{tr}))/2, \quad (3)$$

where  $t = |t|e^{i\theta_t}$ ,  $r = |r|e^{i\theta_r}$ , and  $\Delta_{tr} = \theta_t - \theta_r$  and quantum mechanical averaging is performed with initial state (1). We note that averaging of any contributions containing noise operators is equal to zero.<sup>13</sup> Assuming  $|r| = |t|$ , (2) and (3) simplify as

$$p_c = |t|^2(1 + \cos(\varphi - \Delta_{tr})), \quad (4)$$

$$p_d = |t|^2(1 + \cos(\varphi + \Delta_{tr})). \quad (5)$$

In the case of a lossless beam splitter where we can put  $|r| = |t| = 1/\sqrt{2}$  and  $\Delta_{tr} = \pm\pi/2$ , the probabilities  $p_c$  and  $p_d$  oscillate (with continuous modulation of  $\varphi$ ) out of phase—a well-known single photon interference effect. On the contrary, for an ideal lossy beam splitter with  $|r| = |t| = 1/2$  and  $\Delta_{tr} = \pm\pi$ , the probabilities  $p_c$  and  $p_d$  oscillate in phase, both varying in the range of 0 – 0.5 with total detection, or total transmission probability  $p$ , given by

$$p \equiv p_c + p_d = (1 - \cos \varphi)/2. \quad (6)$$

From the above quantum mechanical analysis, we conclude that for  $\varphi = \pm\pi$  the transmission probability (6) is equal to one and the photon passes through the absorber without losses, while for  $\varphi = 0$  the transmission probability is equal to zero and the photon is absorbed deterministically.

In this work, we demonstrate that regimes of coherent absorption and coherent transmission can be attained in a fully fiberized single mode polarization maintaining fiber quantum network as presented in Fig. 1(a). Heralded single photons at a wavelength of 810 nm are produced via degenerate spontaneous parametric downconversion in a beta-barium borate (BBO) crystal, which is pumped by a CW laser at a wavelength of 405 nm. Detection of an idler photon by avalanche photodiode h (APD-h) heralds the presence of a signal photon in the Mach-Zehnder interferometer containing metamaterial absorber. A piezoelectric fiber stretcher, placed at the bottom arm of the interferometer, is used as a phase modulator to produce phase delay  $\varphi$  between different arms of the interferometer.

A few different ways to manufacture a coherent absorber in the fiber environment were proposed, including encapsulated plasmonic metamaterial,<sup>11</sup> moderately doped fiber in a cavity formed by fiber-Bragg grating mirrors,<sup>15</sup> and chromium layer deposited on the fiber tip.<sup>16</sup> Here we follow the work presented in Ref. 11 and manufacture a plasmonic packaged metadvice, which provides nanostructure design flexibility in a subwavelength film. The absorber, designed as an ideal lossy beam splitter,<sup>2</sup> was manufactured on a 50 nm thick gold film deposited on the cleaved end facet of the fiber [Fig. 1(b)]. The metamaterial nanostructure consisting of a two-dimensional array of asymmetric split-ring resonators [inset in Fig. 1(b)] was carved over a

$30 \times 30 \mu\text{m}^2$  area covering the core of the fiber by focused ion-beam milling. The fiber with deposited metamaterial was then mounted with glass fiber ferrules into a metal housing in such a way that the metamaterial symmetry axis was aligned to the slow axis of the fibers. The resulting metadvice package, shown in inset of Fig. 1(a), was placed in the middle of the interferometer. The optical properties of the metadvice perform as follows at the wavelength of operation (810 nm): transmission  $\approx 20\%$ , reflection metamaterial (bare fiber) side  $\approx 10$  (6)%, and absorption metamaterial (bare fiber) side  $\approx 70$  (74)%. We note that these values include the inner losses in the metamaterial package due to fiber-to-fiber coupling, and actual transmission and reflection of the metamaterial are higher. Similar structures<sup>4,17</sup> reveal that the performance of the metamaterial is broadband without significant changes around the wavelength of interest.

Generally, fiber interferometers require active phase stabilization since they are sensitive to thermally induced fiber-length fluctuations.<sup>18</sup> In a number of experiments with single photons,<sup>19</sup> stabilization was achieved by introducing a feedback loop consisting of (1) reference laser at different wavelengths which probes the same fiber paths as single photons, (2) multiplexer, demultiplexer and optical filters, (3) photodetector for laser power fluctuation measurement, and (4) additional phase modulator to compensate the fiber length drift. Nevertheless, we were able to perform proof-of-principle experiments without any active stabilization by reducing the noise amplitude and bandwidth. This was achieved by winding the fibers around the loop of small radius so that both interferometer arms experience the same temperature fluctuations and by carefully isolating the setup. Moreover, we refined the results by reference-based postselection, where data are acquired within time intervals shorter than the characteristic phase fluctuation time, and the phase of each phase cycle is determined based on characteristic inflection points. Note that the deterministic control of single-photon absorption probability would still require active stabilization as elaborated elsewhere.<sup>20</sup>

The reference-based postselection technique is illustrated in Fig. 2. The length of one arm of the interferometer is periodically modulated with a frequency that is higher than characteristic frequency of the fluctuation spectrum. The modulation amplitude exceeds two wavelengths of light [Fig. 2(a)], and at each cycle the interferometer reaches the condition of perfect absorption [filled points in Fig. 2(b)] twice, while the acquisition time (20 ms) of each point in Fig. 2(b) is much smaller than the period of oscillation ( $\sim 440$  ms). In the absence of fluctuations, the time interval  $\tau_i$  between two points corresponding to perfect absorption is constant and equal to the expected value  $\tau_0$  [Fig. 2(b)]. The data obtained during such intervals are unlikely to be strongly affected by the fluctuation and are used to characterize the photon absorption. In the presence of low-frequency fluctuations, the time interval fluctuates indicating the untrustworthy parts of the data. In experiment, the data are postselected after recording a large number of modulation cycles (around 200). Further, the coincidence counts between detectors APD-h and APD-c (APD-d), recorded during noise-free intervals (around 75), is used to characterize the probability of heralded single photon to take output C (D).

To validate the efficiency of the reference-based postselection technique, we recorded the interference fringes of output C without [Fig. 3(a)] and with [Fig. 3(b)] data processing. While standard deviation, which is mostly defined by Poisson statistics of incoming photon flux (in average, around 23 photons per detection window of 20 ms),

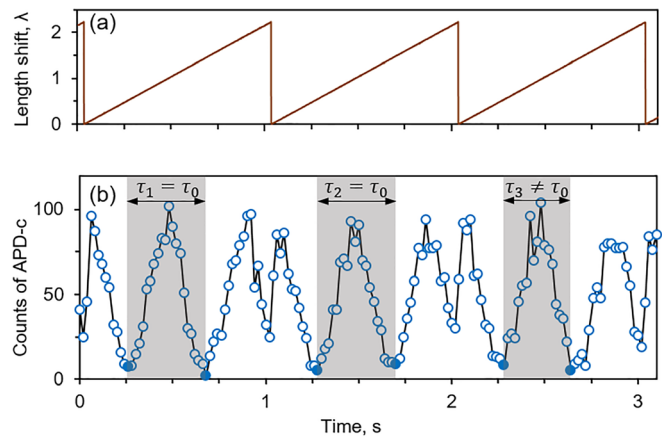


**FIG. 2.** Reference-based postselection technique. (a) Fiber-stretcher periodically induced length shift of one arm of the interferometer showed in photon wavelength units ( $\lambda = 810$  nm). (b) Total single photon counts measured at the detector APD-c. Minima corresponding to the coherent perfect absorption regime (filled dots) within each fiber-stretcher cycle are used as references. The time intervals  $\tau_i$  between these points (shaded regions) are compared with the expected value  $\tau_0$  in the absence of noise. Time intervals  $\tau_i$  close to  $\tau_0$  are likely to be not affected by thermal fluctuations of the interferometer and are used for further data analysis.

remains the same, the visibility of modulation is increased by 10%. Next, by applying postselection, we demonstrate the quantum regimes of total absorption and total transmission in fiber network. We measure the probabilities  $p_c$  and  $p_d$  of detecting a heralded single photon

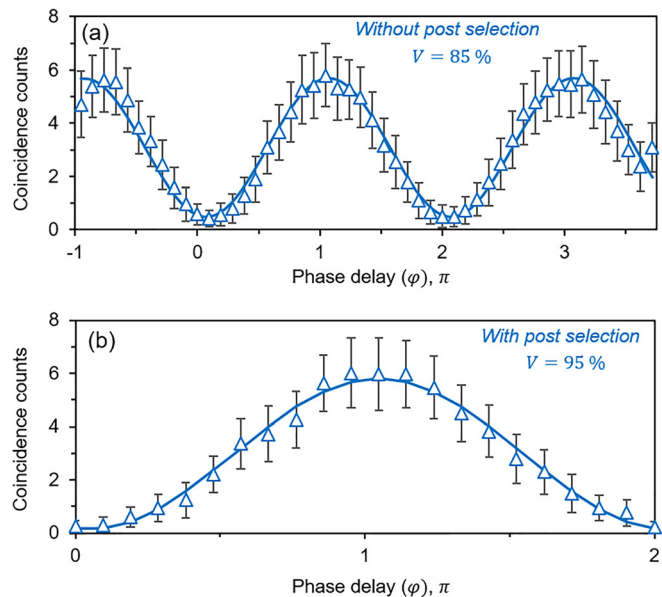


**FIG. 3.** Implementation of reference-based postselection technique. Coincidence counts between detectors APD-c and APD-h without (a) and with (b) postselection. The visibility  $V$  is shown for each fitting curve (solid lines) and improved by 10% after implementation of data processing. Fitting is done according to Eqs. (4)–(6). Side points in (a) are not taken into account for fitting since phase modulation has a jump around these points [Fig. 2(a)]. Error bars are defined by Poisson distribution of photon flux and cannot be improved by data postselection.

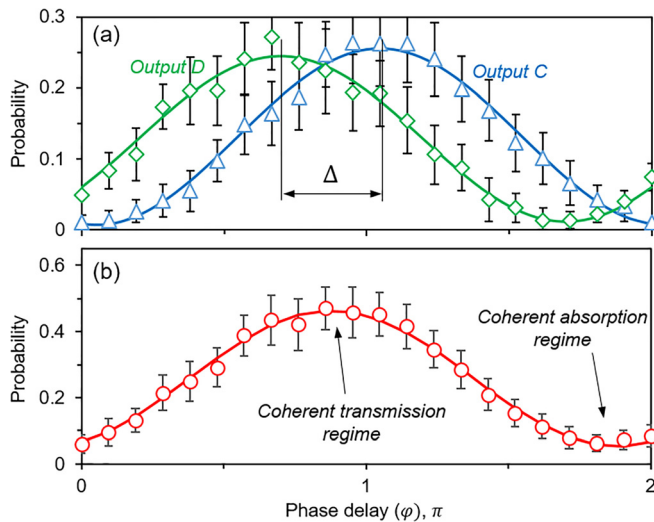


**FIG. 4.** Single-photon coherent absorption. (a) Measured probabilities of the heralded photons, passing through the metamaterial absorber, to take output C (triangles) and output D (rhombi) and to be detected by the detectors APD-c and APD-d, respectively, in dependence on the phase delay  $\varphi$  between two arms of the interferometer. (b) Total single-photon transmission probabilities (circles) in dependence on the phase delay  $\varphi$ . All lines are data fitting according to Eqs. (4)–(6).

at outputs C and D of the metamaterial absorber [Fig. 4(a)]. By scanning the phase shift  $\varphi$ , we observe periodic close to in-phase oscillation of probabilities in good agreement with (6). The phase shift  $\Delta = \pi/3$  between  $p_c$  and  $p_d$  corresponds to non ideal parameters of the absorber and to asymmetry in the metamaterial package design, since light coming from opposite sides of the metamaterial absorber experiences different interfaces. The total probability  $p$  of the heralded single photon detection [Fig. 4(b)] is modulated between 0.05 and 0.46 with the lowest (highest) value corresponding to coherent perfect absorption (transmission) regimes. Reduction of the modulation amplitude of  $p_c$ ,  $p_d$ , and  $p$  is mainly attributed to fiber-to-fiber coupling losses inside the metamaterial package. Nevertheless, this does not affect the visibility of the curves, which is higher than 90% for  $p_c$  and  $p_d$  and equals to 80% for  $p$ .

Interference fringe visibility demonstrated by reference-based postselection data processing is identical to visibility shown in free space experiments,<sup>4,5</sup> where the total single-photon transmission probability  $p$  varied in the range between 0.1 and 0.9. This clearly indicates that metamaterial coherent absorbers fabricated in fiber environment are able to carry the functionality of those implemented in a free space allowing quantum light manipulation in coherent networks including single-photon switching, filtering, and measurement with applications in coherent quantum computation and quantum communication.

It is worth noting that demonstrated coherent optical fiber network can be extended for remote absorption control with polarization entangled photons<sup>5</sup> and high-probability two-photon absorption of bosonic pairs<sup>10</sup> or NOON-states<sup>6</sup> and can be used as a part of a large multiport network.<sup>21</sup> Furthermore, implementation of CPA in the quantum regime at telecom optical wavelength bands will open the ways toward quantum light processing at long distances.

In summary, we have demonstrated continuous control over single-photon absorption probability in a fully fiberized quantum network with a high visibility. A coherent perfect absorber was manufactured directly in the fiber environment by fabrication of plasmonic metamaterial on a fiber end facet. To overcome fiber length thermal fluctuations, we developed a simple data postprocessing procedure which uses the total counts of single photon detector as a reference. Demonstrated effect can find applications in manipulation of single-photon, entangled, weak coherent, and NOON states of light in fiber quantum networks compatible with telecom technologies.

This work was supported by the Singapore A\*STAR QTE program (No. SERC A1685b0005), the Singapore Ministry of Education (No. MOE2016-T3-1-006 (S)), and the UK's Engineering and Physical Sciences Research Council (Grant No. EP/M009122/1).

## REFERENCES

- Y. D. Chong, L. Ge, H. Cao, and A. D. Stone, *Phys. Rev. Lett.* **105**, 053901 (2010); W. Wan, Y. D. Chong, L. Ge, H. Noh, A. D. Stone, and H. Cao, *Science* **331**, 889 (2011); D. G. Baranov, A. Krasnok, T. Shegai, A. Alu, and Y. D. Chong, *Nat. Rev. Mater.* **2**, 17064 (2017).
- J. F. Zhang, K. F. MacDonald, and N. I. Zheludev, *Light Sci. Appl.* **1**, e18 (2012).
- X. Fang, M. L. Tseng, J. Y. Ou, K. F. MacDonald, D. P. Tsai, and N. I. Zheludev, *Appl. Phys. Lett.* **104**, 141102 (2014).
- T. Roger, S. Vezzoli, E. Bolduc, J. Valente, J. J. F. Heitz, J. Jeffers, C. Soci, J. Leach, C. Couteau, N. I. Zheludev, and D. Faccio, *Nat. Commun.* **6**, 7031 (2015).
- C. Altuzarra, S. Vezzoli, J. Valente, W. B. Gao, C. Soci, D. Faccio, and C. Couteau, *ACS Photonics* **4**, 2124 (2017).
- T. Roger, S. Restuccia, A. Lyons, D. Giovannini, J. Romero, J. Jeffers, M. Padgett, and D. Faccio, *Phys. Rev. Lett.* **117**, 023601 (2016).
- A. Ü. C. Hardal and M. Wubs, *Optica* **6**, 181 (2019).
- S. Zanotto, F. P. Mezzapesa, F. Bianco, G. Biasiol, L. Baldacci, M. S. Vitiello, L. Sorba, R. Colombelli, and A. Tredicucci, *Nat. Phys.* **10**, 830 (2014).
- D. Zhang, X.-Q. Luo, Y.-P. Wang, T.-F. Li, and J. Q. You, *Nat. Commun.* **8**, 1368 (2017).
- B. Vest, M. C. Dheur, E. Devaux, A. Baron, E. Rousseau, J. P. Hugonin, J. J. Greffet, G. Messin, and F. Marquier, *Science* **356**, 1373 (2017).
- A. Xomalis, I. Demirtzioglou, E. Plum, Y. M. Jung, V. Nalla, C. Lacava, K. F. MacDonald, P. Petropoulos, D. J. Richardson, and N. I. Zheludev, *Nat. Commun.* **9**, 182 (2018).
- S. Thongrattanasiri, F. H. L. Koppens, and F. J. G. de Abajo, *Phys. Rev. Lett.* **108**, 047401 (2012).
- S. M. Barnett, J. Jeffers, A. Gatti, and R. Loudon, *Phys. Rev. A* **57**, 2134 (1998).
- J. Jeffers, *J. Mod. Opt.* **47**, 1819 (2000).
- A. K. Jahromi, A. Van Newkirk, and A. F. Abouraddy, *IEEE Photonics J.* **10**, 1 (2018).
- A. Goodarzi, M. Ghanaatshoar, and M. Mozafari, *Sci. Rep.* **8**, 15340 (2018).
- A. Xomalis, I. Demirtzioglou, Y. Jung, E. Plum, C. Lacava, P. Petropoulos, D. J. Richardson, and N. I. Zheludev, *Appl. Phys. Lett.* **113**, 051103 (2018).
- T. Musha, J. Kamimura, and M. Nakazawa, *Appl. Opt.* **21**, 694 (1982).
- S. B. Cho and T. G. Noh, *Opt. Express* **17**, 19027 (2009); G. B. Xavier and J. P. von der Weid, *Opt. Lett.* **36**, 1764 (2011); P. Toliver, J. M. Dailey, A. Agarwal, and N. A. Peters, *Opt. Express* **23**, 4135 (2015).
- S. Yanikgonul, R. Guo, A. Xomalis, A. N. Vetlugin, G. Adamo, C. Soci, and N. I. Zheludev, "Phase stabilization of a coherent fibre network by single-photon counting" (to be published).
- K. Pichler, M. Kühmayer, J. Böhm, A. Brandstötter, P. Ambichl, U. Kuhl, and S. Rotter, *Nature* **567**, 351 (2019); S. Fan, W. Suh, and J. D. Joannopoulos, *J. Opt. Soc. Am. A* **20**, 569 (2003).